Collect. Czech. Chem. Commun.; doi:10.1135/cccc2011179

Supplementary Information

WHY DO DISILANES FAIL TO FLUORESCE?

Matthew MACLEOD[a] and Josef MICHL[a,b]

[a]*Department of Chemistry and Biochemistry, University of Colorado, Boulder, Colorado 80309, USA, and Institute of Organic Chemistry and Biochemistry,* [b]*Academy of Sciences of the Czech Republic, Flemingovo nám., 2, 166 10 Praha 6, Czech Republic*

Table of Contents

Supplementary Information

Vibrational analysis of the S_1 stationary points was carried out to investigate the nature of the stationary points. For **1a**, methods which did not utilize the PBE0 functional indicated only the lowest vibrational frequency on the S_1 surface to be imaginary (Table I).

Table I. Lowest vibrational frequency for the stationary points **1a-z** on the S_1 surface.

Structure	Method	Lowest Frequency Vibration
1a	PBE0/TZVP	27.8
	PBE0/aug-cc-PVDZ	33.0
	PBE0/cc-PVTZ	28.8
	B3LYP/TZVP	*i*29.8
	BHLYP/TZVP	*i*19.2
	RIADC(2)/TZVP	*i*31.8
	RICC2/TZVP	*i33.0*
1b	PBE0/TZVP	21.9
	B3LYP/TZVP	22.2
	B3LYP/aug-cc-pVDZ	26.1
	BHLYP/TZVP	18.9
	RIADC(2)/TZVP	26.7
	RIADC(2)/Def2-TZVP-mD	23.4
	RICC2/TZVP	29.8
1c	B3LYP/TZVP	38.1
1d	B3LYP/aug-cc-pVDZ	37.6
1z	B3LYP/TZVP	27.6

A graphical summary of the various optimizations carried out on **1** is shown in Figure 1.

For comparison, the geometries of the neutral ground state equilibrium structure **1** and relaxed radical cation $\mathbf{1}^+$ are listed in Table II. The structures of the radical cation and the Rydberg minimum **1d** are similar.

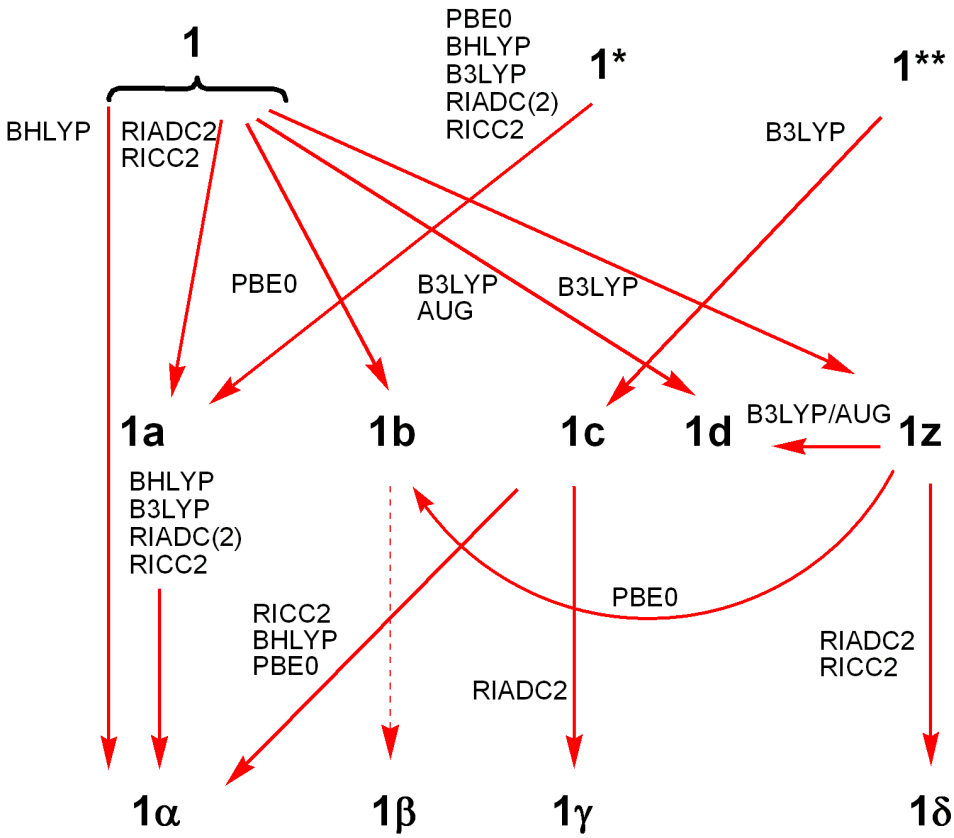

Figure 1. Schematic of the valence excited state (S_1) optimization results for hexamethyldisilane. The method is listed to the left of or above the arrow. Dashed arrow indicates that a distortion is needed.

Table II. Geometrical parameters for **1** and the radical cation, $\mathbf{1}^{+}$. Bond lengths are in Å and valence angles in degrees.

Structure	∠CSiC / deg	∠ CSiSi / deg	SiSi / Å	SiC / Å
1 RIMP2/Def2-TZVP D_{3d}	108.8 108.8 108.8 108.8 108.8 108.8	110.1 110.1 110.1 110.1 110.1 110.1	2.353	1.886 1.886 1.886 1.886 1.886 1.886
1 B3LYP/aug-cc-pVDZ D_{3d}	108.6 108.6 108.6 108.6 108.6 108.6	110.3 110.3 110.3 110.3 110.3 110.3	2.375	1.907 1.907 1.907 1.907 1.907 1.907
1+ RIUMP2/aug-cc-pVDZ D_3	116.2 116.2 116.2 116.2 116.2 116.2	101.5 101.5 101.5 101.5 101.5 101.5	2.666	1.853 1.853 1.853 1.853 1.853 1.853
1+ UB3LYP/aug-cc-pVDZ D_3	115.7 115.7 115.7 115.7 115.7 115.7	102.1 102.1 102.1 102.1 102.1 102.1	2.717	1.877 1.877 1.877 1.877 1.877 1.877

Geometries for the S_0-S_1 funnel structures are included in Table III. These structures are very approximate due to the single reference method used for optimizations, as can be seen by the high diagnostic values[12] in Table IV. The S_1 minima, on the other hand, are well described by the single reference methods used in this work.

Table III. S_0-S_1 funnel structures (RIADC(2)/TZVP) for hexamethyldisilane.

Structure	∠CSiC / deg	∠ CSiSi / deg	SiSi / Å	SiC / Å
1α C_1	107.5 108.3 110.4 155.4 92.9 91.5	107.3 80.0 114.0 109.3 83.0 146.2	2.646	1.898 1.895 1.896 1.965 1.939 1.982
1α[a] C_1	91.3 160.6 92.4 110.1 110.2 105.3	154.6 85.1 83.5 109.3 108.0 113.9	2.552	1.950 1.995 1.983 1.897 1.888 1.888
1β C_s	110.0 111.6 111.6 167.6 91.4 91.4	105.5 109.1 109.1 85.5 85.5 146.9	2.647	1.887 1.887 1.883 1.978 1.978 1.919
1γ C_1	96.8 119.8 73.7 108.4 107.9 108.8	157.0 83.7 97.8 111.6 99.5 119.9	2.477	1.922 2.525 1.922 1.890 1.887 1.904
1δ C_3	115.7 114.8 115.7 106.7 106.1 107.1	76.9 77.2 77.0 112.7 112.6 111.3	3.471	1.810 1.805 1.811 1.941 1.941 1.944

[a]This funnel was obtained from the BHLYP/TZVP TDA optimization of **1a**, distorted along the imaginary vibration.

Table IV. D_1 and D_2 diagnostics (calculated for S_0 with the RIADC(2)/TZVP method) for hexamethyldisilane minima and S_0-S_1 funnels.

Structure	Method	D_1	D_2
1a	PBE0	0.023	0.21
	B3LYP	0.023	0.21
	BHLYP	0.023	0.21
	RIADC(2)	0.025	0.22
	RICC2	0.025	0.21
1b	PBE0	0.025	0.25
	B3LYP	0.025	0.25
	BHLYP	0.027	0.25
	RIADC(2)	0.062	0.26
	RIADC(2)[a]	0.032	0.28
	RICC2	0.030	0.26
1c	B3LYP	0.027	0.30
1d	B3LYP[a]	0.022	0.22
1z	B3LYP	0.025	0.26
1α	RIADC(2)	0.110	0.51
1β	RIADC(2)	0.030	0.23
1γ	RIADC(2)	0.055	0.38
1δ	RIADC(2)	0.099	0.50

[a] This structure originates from the RIADC(2)/Def2-RZVP-mD S_1 optimization.

The μ parameter used in the LC-BLYP calculations was optimized to reproduce previous estimates of the ground to σπ* excitation energy. These values are listed in Table V.

Table V. Vertical absorption energy (E_{VA}) and oscillator strength (f).

Structure	Method	State	E_{VA} / cm^{-1}	f
1	B3LYP/Def2TZVP	$1E_u$ σπ*	52 660	0.143
1	B3LYP-AC/cc-pVTZ[a]	$1E_u$ σπ*	51 990	0.146
1	CAMB3LYP/Def2TZVP	$1E_u$ σπ*	55 400	0.178
1	LCBLYP/Def2TZVP	$1E_u$ σπ*	55 330	0.173
1	LCBLYP/Def2TZVP[b]	$1E_u$ σπ*	52 340	0.144
1	RICC2/Def2TZVP	$1E_u$ σπ*	56 740	0.214
1	Experiment[c]	$1E_u$ σπ*	52 300	0.151

[a] This calculation is similar (functional and basis set) to previous calculations on **1**[3]. [b] The μ parameter is set to 0.23 a_0^{-1} for this LC-BLYP calculation, as opposed to the default value, 0.33 a_0^{-1}. [c] The experimental E_{VA} value is for **1** at 77 K[4].

The blue and green minima can easily rearrange to find nearby S_0-S_1 funnel regions. The geometrical distortions necessary for these processes are shown in Figure 2.

While the **1α** and **1β** S_0-S_1 funnels have similar structures for Si_2Me_6, the geometrical parameters are sensitive to the disilane substituents. For example, the **1α** disilane analog (Si_2H_6) funnel structures are given in Figure 3 and has a largely contracted H-Si-Si valence angle (48.4°), which is smaller than the equivalent angles in both the **1α** and **1β** funnels (83.0° and 85.5°, respectively). No S_1 minima were located for Si_2H_6.

Simple calculations which involved relaxed scan of the potential energy surface along a specified coordinate were carried out to estimate the barrier height of the minimum to funnel regions. For **1a,** this involved a scan of the C(2)-Si(1)-C(3) valence angle (while all other variables were optimized, Table VI) and for **1b**, it involved a scan of the C(2)-Si(1)-Si(2) valence angle, again while optimizing all other variables (Table VII).

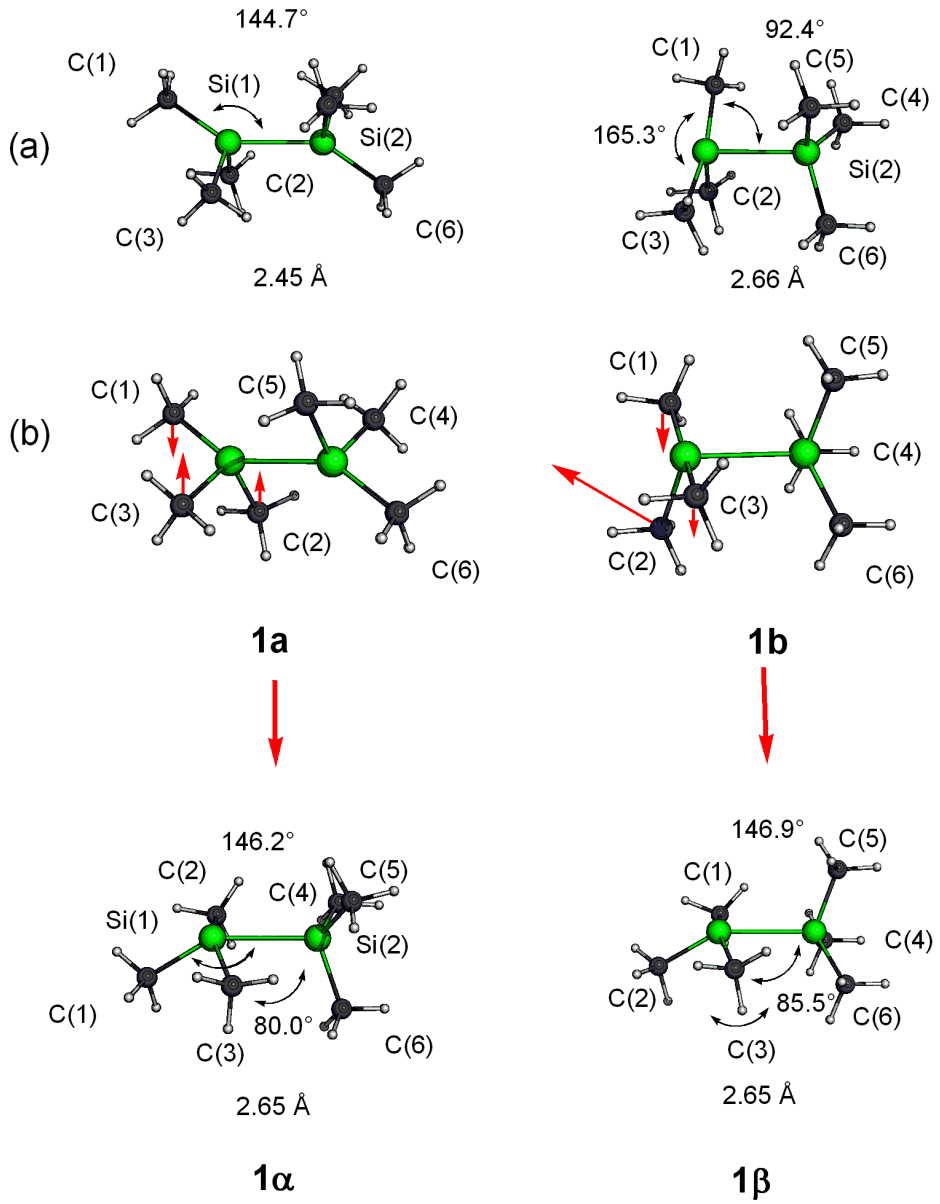

Figure 2. Schematic for the **1a** and **1b** structural rearrangement to the funnels **1α** and **1β**, respectively. Geometries are shown for the minima, (a), and the forces (red arrows) needed for rearrangement to the RIADC(2)/TZVP funnels, (b).

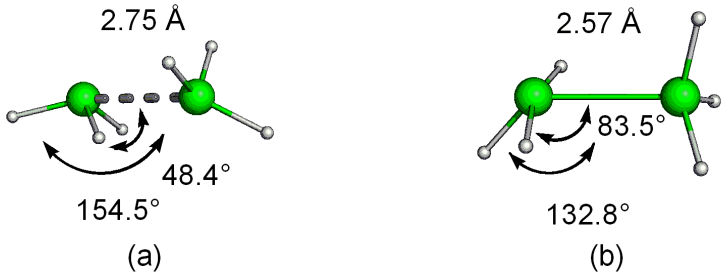

Figure 3. Parent disilane analogs of the **1α** and **1β** S_0-S_1 funnel structures (a) and (b), respectively. The Si-Si bond length is indicated as well as various H-Si-Si valence angles (in degrees).

Table VI. Relaxed scan along the C(2)-Si(1)-C(3) valence angle on the S_1 surface of **1a** (all other geometrical parameters optimized). Energies calculated with the TDDFT/TDA (PBE0/TZVP) method.

∠ C(2)Si(1)C(3) / deg	E_{VE} / cm^{-1}	f	$\Delta S_{0Min}S_0$ / cm^{-1}	$\Delta S_{1Min}S_1$ / cm^{-1}
95.0	26 200	0.052	2 210	810
100.0	26 760	0.060	1 190	350
105.0	27 210	0.063	480	80
110.2	27 530	0.066	70	0
111.0	27 570	0.066	30	1
111.8	27 600	0.066	8	5
112.0	27 600	0.066	4	6
112.4	27 610	0.065	0	8
112.6	27 610	0.065	4	10
112.8	27 590	0.064	20	11
115.0	26 560	0.052	960	-80
120.0	25 770	0.047	1 650	-180
125.0	24 570	0.041	2 820	-210
135.0	20 780	0.028	6 560	-270
138.0	18 840	0.023	8 410	-340
140.0	16 940	0.020	10 220	-440
141.0	15 420	0.018	11 660	-520
142.0	2 510	0.002	24 080	-1 000

Table VII. Relaxed scan along the C(2)-Si(1)-Si(2) valence angle on the S_1 surface of **1b** (all other geometrical parameters were optimized). Energies are calculated with the TDDFT/TDA (PBE0/TZVP) method.

∠ C(1)Si(1)Si(2) / deg	E_{VE} / cm^{-1}	f	$\Delta S_{0Min}S_0$ / cm^{-1}	$\Delta S_{1Min}S_1$ / cm^{-1}
80.4	17 590	0.008	2 900	990
81.6	17 870	0.008	2 480	850
85.8	18 550	0.009	1 450	500
92.7	19 252	0.010	390	160
102.5	19 500	0.011	0	0
112.9	18 140	0.014	1 460	100
123.8	16 310	0.012	3 420	240
124.5	16 140	0.012	3 610	250
126.0	15 750	0.012	4 030	280
128.0	15 160	0.011	4 650	310
130.0	14 450	0.011	5 380	340
132.0	13 580	0.010	6 270	350
134.0	12 410	0.009	7 450	350
136.0	354	0.000	17 530	-1 610

The composition of the **1a**,**1b** and **1z** hypervalent nonbonding orbitals is given in Table VIII. The exact composition of the green minimum **1b** nonbonding orbital varied depending on which structure was analyzed. Analysis of the ab initio structures showed higher occupation numbers in the nonbonding orbital than in the TDDFT structures. The latter structures seemed to favor moving electron density into the $\sigma^*_{Si\text{-}C}$ orbitals instead of the fifth valence orbital described in Table VIII.

Table VIII. The blue minimum **1a**, green minimum **1b** and **1z**: Hypervalent nonbonding orbital composition in terms of natural atomic orbitals (NAOs). The NAOs with a weight exceeding 1% are included below. NAO type (valence or Rydberg orbital) is defined by the principal quantum number. NHO analysis was done with the CIS/6-311G(d,p) method.

Structure	%	NAO	Type
1a PBE0/TZVP	6.9 2.5 3.3 50.3 1.1 11.6 21.5 1.2	s s p_z p_z d_{xy} d_{xz} $d_{x^2-y^2}$ d_{z^2}	Val (3s) Ryd (4s) Val (3p) Ryd (4p) Ryd (3d) Ryd (3d) Ryd (3d) Ryd (3d)
1b RIADC(2)/Def2TZVP-mD	1.1 37.9 3.8 23.9 25.5 6.4	s s p_x p_z $d_{x^2-y^2}$ d_{z^2}	Val (3s) Ryd (4s) Val (3p) Ryd (4p) Ryd (3d) Ryd (3d)
1b RICC2/TZVP	5.4 16.1 21.3 5.2 23.4 1.1 18.7 8.4	s s p_x p_z p_z d_{xz} $d_{x^2-y^2}$ d_{z^2}	Val (3s) Ryd (4s) Val (3p) Val (3p) Ryd (4p) Ryd (3d) Ryd (3d) Ryd (3d)
1b BHLYP/TZVP	30.6 4.0 29.5 24.2 9.7	s p_x p_z $d_{x^2-y^2}$ d_{z^2}	Ryd (4s) Val (3p) Ryd (4p) Ryd (3d) Ryd (3d)

1z B3LYP/TZVP	1.1 52.4 4.3 30.7 8.0 2.7	s s p_x p_x $d_{x^2-y^2}$ d_{z^2}	Val (3s) Ryd (4s) Val (3p) Ryd (4p) Ryd (3d) Ryd (3d)

References

1. Janssen, C.; Nielson, I. *Chem. Phys. Lett.* 1998, 290, 423.

2. Nielson, I.; Janseen, C. *Chem. Phys. Lett.* 1999, 310, 568.

3. Piqueras, M. C.; Crespo, R.; Michl, J. *J. Phys. Chem. A* 2008, 112,13095.

4. Casher, D. L.; Tsuji, H.; Sano, A.; Katkevics, M.; Toshimitsu, A.; Tamao, K.; Kubota, M.; Kobayashi, T.; Ottosson, C. H.; David, D. E.; Michl, J. *J. Phys. Chem. A* 2003, 107, 3559.